World Academy of Science, Engineering and Technology
International Journal of Electrical and Computer Engineering
Vol:1, No:1, 2007

Control of Chaotic Dynamical Systems using RBF Networks

Yoichi Ishikawa, Yuichi Masukake, and Yoshihisa Ishida

***Abstract*—**This paper presents a novel control method based on radial basis function networks (RBFNs) for chaotic dynamical systems. The proposed method first identifies the nonlinear part of the chaotic system off-line and then constructs a model-following controller using only the estimated system parameters. Simulation results show the effectiveness of the proposed control scheme.

***Keywords*—**Chaos, nonlinear plant, radial basis function network.

I. Introduction

CHAOS is a special feature of parametric nonlinear dynamical systems. It is usually difficult to accurately predict its future behavior. Recently, a family of artificial neural networks have gotten good results on the prediction and control of the nonlinear plants [1]-[6]. K. S. Narendra *et al.* [3] have proposed identification and control methods of nonlinear dynamical systems using multi-layered perceptron neural networks. On the other, K. B. Kim *et al.* [6] have presented control of chaotic dynamical systems using RBF network approximators and demonstrated its effectiveness. The RBF networks are well known for their stable learning capability and fast training.

In this paper, we propose a design method of model-following controller using RBF networks, which is robust to disturbance and change of system parameters, improving on their basic idea for the control of nonlinear systems. The proposed method is applied to the Duffing and the Lorenz systems and its effectiveness is presented.

II. Problem Statement

Consider a discrete chaotic dynamical system given by

$$\boldsymbol{x}(\boldsymbol{k}+1)=\boldsymbol{A}\boldsymbol{x}(\boldsymbol{k})+\boldsymbol{f}_N[\boldsymbol{x}(\boldsymbol{k})], \tag{1}$$

where $f_N[\boldsymbol{x}(k)]$ is the nonlinear part of the system dynamics. In (1), $\boldsymbol{A}$ is assumed to be known and $f_N[\boldsymbol{x}(k)]$ is unknown but the inputs and outputs can be measured. We rewrite (1) to the system with a scalar control input of the form

$$\boldsymbol{x}(\boldsymbol{k}+1)=\boldsymbol{A}\boldsymbol{x}(\boldsymbol{k})+\boldsymbol{f}_N[\boldsymbol{x}(\boldsymbol{k})]+\boldsymbol{b}\boldsymbol{u}(\boldsymbol{k}), \tag{2}$$

where

$$\boldsymbol{b}=[1\,1\cdots 1]^{\boldsymbol{T}}. \tag{3}$$

Then, we can also define the system output by

$$\boldsymbol{y}_p(\boldsymbol{k})=\begin{bmatrix}1 & 0 & \cdots & 0\\ 0 & 1 & \cdots & 0\\ \vdots & \vdots & \ddots & \vdots\\ 0 & 0 & \cdots & 1\end{bmatrix}\boldsymbol{x}(\boldsymbol{k})=\boldsymbol{x}(\boldsymbol{k}). \tag{4}$$

Let us assume that the difference equation of the reference model for the chaotic system is given by a second-order system

$$\begin{aligned}\boldsymbol{y}_m(\boldsymbol{k}+1)=&-\boldsymbol{a}_{m1}\boldsymbol{y}_m(\boldsymbol{k})-\boldsymbol{a}_{m2}\boldsymbol{y}_m(\boldsymbol{k}-1)\\&+\boldsymbol{b}_{m0}\boldsymbol{r}(\boldsymbol{k})+\boldsymbol{b}_{m1}\boldsymbol{r}(\boldsymbol{k}-1),\end{aligned} \tag{5}$$

where

$\boldsymbol{y}_m(\boldsymbol{k})$: model output,

$\boldsymbol{r}(\boldsymbol{k})$: reference input.

In [3], the error between the model and plant output is defined as

$$\boldsymbol{e}(\boldsymbol{k})=\boldsymbol{y}_m(\boldsymbol{k})-\boldsymbol{y}_p(\boldsymbol{k}), \tag{6}$$

and the design method is based on the condition

$$\lim_{k\to\infty}\boldsymbol{e}(\boldsymbol{k})=0. \tag{7}$$

Then, from the relations (2)-(6), we obtain

$$\begin{aligned}\boldsymbol{b}\boldsymbol{u}(\boldsymbol{k})=&-\boldsymbol{a}_{m1}\boldsymbol{y}_p(\boldsymbol{k})-\boldsymbol{a}_{m2}\boldsymbol{y}_p(\boldsymbol{k}-1)\\&+\boldsymbol{b}_{m0}\boldsymbol{r}(\boldsymbol{k})+\boldsymbol{b}_{m1}\boldsymbol{r}(\boldsymbol{k}-1)\\&-\boldsymbol{A}\boldsymbol{x}(\boldsymbol{k})-\boldsymbol{f}_N(\boldsymbol{k}),\end{aligned} \tag{8}$$

where $f_N(k)\equiv f_N[\boldsymbol{x}(k)]$. In (8), due to the non-presence of an integrator, it is considered that the system is prone to the offsets caused by the step disturbance.

Now, let us assume that at the steady state the following condition is satisfied:

$$\boldsymbol{e}(\boldsymbol{k}+1)=\boldsymbol{e}(\boldsymbol{k}). \tag{9}$$

In this case, if $e(0)\neq 0$, then $\lim_{k\to\infty}\boldsymbol{e}(\boldsymbol{k})\neq 0$. Furthermore, it is not guaranteed about the stability at the steady state. These problems will be solved later. From (9)

$$\boldsymbol{y}_m(\boldsymbol{k}+1)-\boldsymbol{y}_p(\boldsymbol{k}+1)=\boldsymbol{y}_m(\boldsymbol{k})-\boldsymbol{y}_p(\boldsymbol{k}), \tag{10}$$

By substituting (2) and (5) into (10) and replacing $y_m(k)$ with $y_p(k)$, we have

$$\begin{aligned}\boldsymbol{b}\boldsymbol{u}(\boldsymbol{k})=&\,\boldsymbol{b}\boldsymbol{u}(\boldsymbol{k}-1)-\boldsymbol{a}_{m1}\boldsymbol{y}_p(\boldsymbol{k})-\boldsymbol{a}_{m2}\boldsymbol{y}_p(\boldsymbol{k}-1)\\&+\boldsymbol{b}_{m0}\boldsymbol{r}(\boldsymbol{k})+\boldsymbol{b}_{m1}\boldsymbol{r}(\boldsymbol{k}-1)\\&-\boldsymbol{A}[\boldsymbol{x}(\boldsymbol{k})-\boldsymbol{x}(\boldsymbol{k}-1)]\\&-[\boldsymbol{f}_N(\boldsymbol{k})-\boldsymbol{f}_N(\boldsymbol{k}-1)]-\boldsymbol{y}_p(\boldsymbol{k}).\end{aligned} \tag{11}$$

In the above, due to the appearance of the term $\boldsymbol{b}\boldsymbol{u}(\boldsymbol{k}-1)$, the effect of an integrator operation is expected and it will become robust to change of system parameters. On the other, substituting (11) into (2), we obtain

Manuscript received November 6, 2006. Manuscript accepted December 20, 2006. This research was supported in part by a research grant from SMC Corporation, Japan.

The authors are with the Department of Electronics and Communications, Meiji University, Kawasaki, 214-8571, Japan(e-mail:ishida@isc.meiji.ac.jp).

$$\begin{aligned} y_p(k+1) &= -a_{m1} y_p(k) - a_{m2} y_p(k-1) \\ &\quad + b_{m0} r(k) + b_{m1} r(k-1), \end{aligned} \tag{12}$$

It is clear that the following condition is satisfied for arbitrary initial value $e(0)$.

$$\lim_{k\to\infty} e(k) = 0. \tag{13}$$

Furthermore, the stability of the proposed method is obvious from some simulation experiments.

III. NONLINEARITY COMPENSATION USING RBF NETWORKS

A. RBF Networks

Fig. 1 illustrates RBF networks (RBFNs) with N_i inputs, N_h radial basis functions (RBFs), and N_o outputs. In Fig. 1, each RBF is given by so-called a Gaussian response function:

$$h_i = \exp\left(-\frac{\|x - c_i\|^2}{2\sigma^2}\right), \tag{14}$$

where $x = [x_1, x_2, \cdots, x_{N_i}]^T$ is the input vector, c_i is centroid vector of the i-th RBF, $\|\cdots\|^2$ denotes L_2 norm, and σ is the radius. The output of each RBF, $y_j (j = 1, 2, \cdots, N_0)$, is then given as the linearly weighted sum of h_i, i.e.,

$$y_j = \sum_i h_i w_{ji} \Big/ \sum_i h_i, \tag{15}$$

where

$$W = \begin{bmatrix} w_{11} & w_{12} & \cdots & w_{1N_h} \\ w_{21} & w_{22} & \cdots & w_{2N_h} \\ \vdots & \vdots & \ddots & \vdots \\ w_{N_o1} & w_{N_o2} & \cdots & w_{N_oN_h} \end{bmatrix}^T \tag{16}$$

is called as the weight matrix.

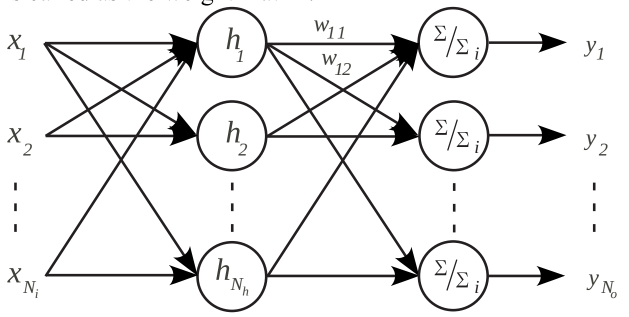

Fig. 1 RBF Networks

B. Design of Approximator

In the design, the function $f_N(k)$ in (1) is replaced with the output $y(k) = [y_1(k), y_2(k), \cdots, y_{N_o}(k)]^T$ of the RBFNs, namely

$$f_N(k) \approx y(k). \tag{17}$$

To estimate the weight matrix W of the RBFNs we apply the singular value decomposition (SVD) [7] instead of applying the conventional least squares. Namely, the following relation is considered:

$$HW = Y \tag{18}$$

with

$$H = \begin{bmatrix} \tilde{h}_1(k-N+1) & \tilde{h}_2(k-N+1) & \cdots & \tilde{h}_{N_h}(k-N+1) \\ \tilde{h}_1(k-N+2) & \tilde{h}_2(k-N+2) & \cdots & \tilde{h}_{N_h}(k-N+2) \\ \vdots & \vdots & \ddots & \vdots \\ \tilde{h}_1(k) & \tilde{h}_2(k) & \cdots & \tilde{h}_{N_h}(k) \end{bmatrix} \in \Re^{N\times N_h},$$

$$Y = \begin{bmatrix} y^T(k-N+1) \\ y^T(k-N+2) \\ \vdots \\ y^T(k) \end{bmatrix} \in \Re^{N\times N_o},$$

where $N > N_h$ and

$$\tilde{h}_i(k) \equiv \frac{h_i(k)}{\sum_i h_i(k)}.$$

Applying the SVD, the matrix H can be rewritten:

$$H = USV^T, \tag{19}$$

where the matrix $U = [u_1, u_2, \cdots, u_N] \in \Re^{N\times N}$ and $V = [v_1, v_2, \cdots, v_{N_h}] \in \Re^{N_h\times N_h}$ are orthogonal to each other such that $U^T U = I_N$ and $V^T V = I_{N_h}$, respectively, and $S = diag(\lambda_1, \lambda_2, \cdots, \lambda_{N_h})$ with $\lambda_1 > \lambda_2 > \cdots > \lambda_{N_h}$. Then, we assume that the last (N_h - r) diagonal entries satisfy the relation $\lambda_{r+1} = \lambda_{r+2} = \cdots = \lambda_{N_h} = 0$, the diagonal matrix S is re-written as

$$S = \begin{bmatrix} \Sigma & 0 \\ 0 & 0 \end{bmatrix}, \tag{20}$$

where $\Sigma = diag(\lambda_1, \lambda_2, \cdots, \lambda_r)$ and $r < N_h$.

Finally, the matrix W can be estimated using the reduced-rank version S_r of the matrix S:

$$S_r = \begin{bmatrix} \Sigma^{-1} & 0 \\ 0 & 0 \end{bmatrix}, \tag{21}$$

$$W = VS_r U^T Y. \tag{22}$$

IV. SIMULATION RESULTS

In the simulation study, the transfer function of the reference model is given in the form of a standard second-order system:

$$G_m(s) = \frac{\omega_m^2}{s^2 + 2\zeta_m \omega_m s + \omega_m^2}, \tag{23}$$

where ω_m = 50[rad/sec] and ζ_m =1. To obtain the difference equation of the reference model in discrete form, we used the zero-order hold method [8]. The sampling interval was 10 [msec]. Then, the coefficients of the reference model were a_{m1} = -1.213, a_{m2} = 0.368, b_{m0} = 0.090, and b_{m1} = 0.065, respectively. Throughout the simulation study, the reference input $r(k)$ (with a total of 100 samples) was fixed as

$$\boldsymbol{r}(\boldsymbol{k}) = \begin{cases} 1: \text{if } \boldsymbol{k} = 0,1,\cdots,24 \\ \quad \text{and } \boldsymbol{k} = 50,51,\cdots,74, \\ 0: \text{otherwise}. \end{cases} \tag{24}$$

To study the immunity from the disturbance, the step disturbance at k = 40 with the magnitude $d(40)$ = 0.05 is intentionally added to the plant input $u(k)$. The structure of the proposed control system by SIMULINK is presented in Fig. 2.

A. Example 1: Duffing System

The continuous dynamics of the chaotic Duffing system is given by

$$\dot{\boldsymbol{x}}(\boldsymbol{t}) = \begin{bmatrix} 0 & 1 \\ 1.1 & -0.4 \end{bmatrix} \boldsymbol{x}(\boldsymbol{t}) + \begin{bmatrix} 0 \\ -\boldsymbol{x}_1^3(\boldsymbol{t}) + 1.8\cos(1.8\boldsymbol{t}) \end{bmatrix}. \tag{25}$$

Fig. 3 illustrates an example of the trajectory Duffing system.

Discretizing (25) with the sampling interval T_s = 10[msec], we have

$$\boldsymbol{x}(\boldsymbol{k}+1) = \begin{bmatrix} 1.0001 & 0.0100 \\ 0.0110 & 0.9961 \end{bmatrix} \boldsymbol{x}(\boldsymbol{k}) + \begin{bmatrix} 0 \\ 0.01\{-\boldsymbol{x}_1^3(\boldsymbol{k}) + 1.8\cos(1.8\boldsymbol{k})\} \end{bmatrix}. \tag{26}$$

Off-line identification for the nonlinear part of the system is first performed. For the approximator of the Duffing system, the structure of the RBFNs is summarized in Table I.

TABLE I
STRUCTURE OF THE RBFNS FOR THE DUFFING SYSTEM

Number of hidden nodes	30
Number of inputs, outputs	2, 2
Number of clustering samples	1000
Off-line training iteration	10000

The simulation result for $x_1(k)$ of this tracking control is illustrated in Fig. 4, where the initial state was $x(0) = [1\ 1]^T$. The dotted and solid lines show the model and plant outputs, respectively.

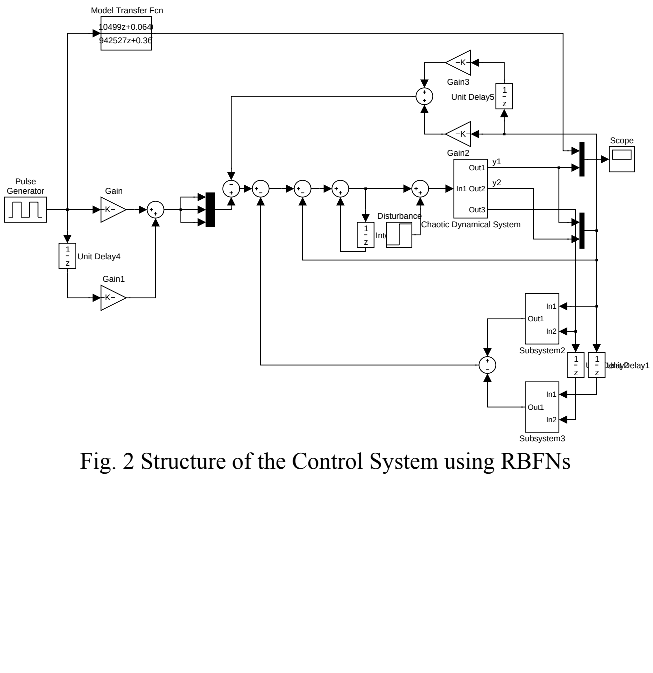

Fig. 2 Structure of the Control System using RBFNs

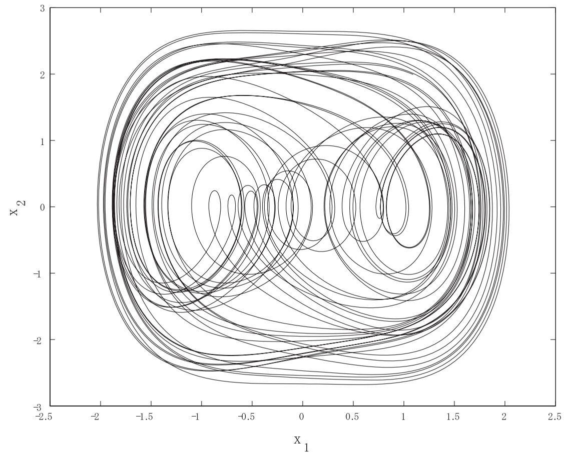

Fig. 3 A plot example of the trajectory Duffing system

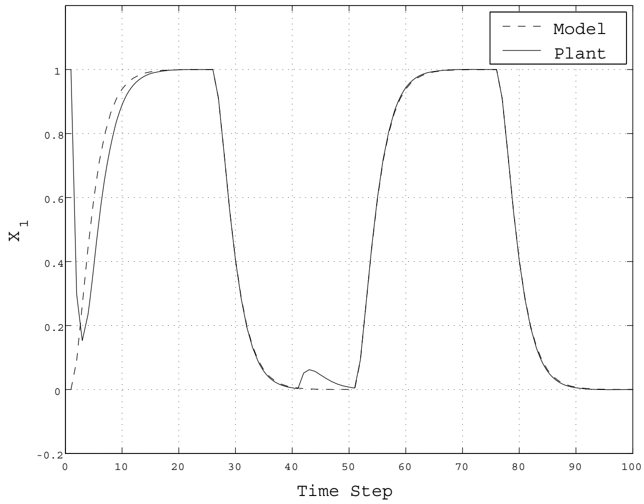

Fig. 4 Tracking Control of the Duffing system

B. Example 2: Lorenz System

The continuous dynamics of the chaotic Lorenz system is given by

$$\dot{\boldsymbol{x}}(\boldsymbol{t}) = \begin{bmatrix} -10 & -10 & 0 \\ 28 & -1 & 0 \\ 0 & 0 & 1 \end{bmatrix} \boldsymbol{x}(\boldsymbol{t}) + \begin{bmatrix} 0 \\ -\boldsymbol{x}_1(\boldsymbol{t})\boldsymbol{x}_3(\boldsymbol{t}) \\ \boldsymbol{x}_1(\boldsymbol{t})\boldsymbol{x}_2(\boldsymbol{t}) \end{bmatrix}. \tag{27}$$

Fig. 5 illustrates an example of the trajectory Lorenz system. Then, the discrete form of the Lorenz system is given by

$$\boldsymbol{x}(\boldsymbol{k}+1) = \begin{bmatrix} 0.9179 & 0.0951 & 0 \\ 0.2663 & 1.0035 & 0 \\ 0 & 0 & 0.9736 \end{bmatrix} \boldsymbol{x}(\boldsymbol{k}) + \begin{bmatrix} 0 \\ -0.01\boldsymbol{x}_1(\boldsymbol{k})\boldsymbol{x}_3(\boldsymbol{k}) \\ 0.01\boldsymbol{x}_1(\boldsymbol{k})\boldsymbol{x}_2(\boldsymbol{k}) \end{bmatrix}. \tag{28}$$

For the Lorenz system, the RBFNs summarized in Table II was used as the approximator of the nonlinear part. The simulation result for $x_2(k)$ of this tracking control is presented in Fig. 6, where the initial state was $x(0) = [1\ 1\ -1]^T$.

TABLE II
STRUCTURE OF THE RBFNS FOR THE LORENZ SYSTEM

Number of hidden nodes	30
Number of inputs, outputs	3, 3
Number of clustering samples	5000
Off-line training iteration	15000

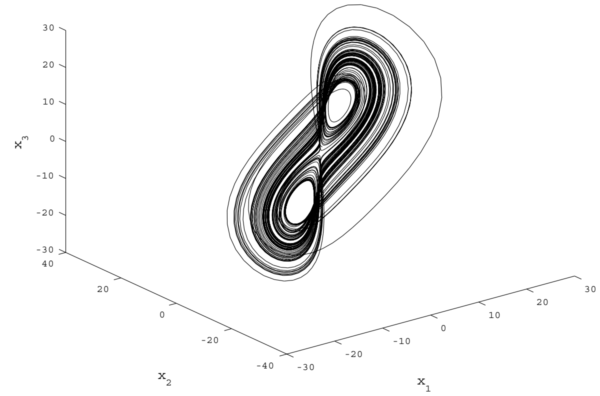

Fig. 5 A plot example of the trajectory Lorenz system

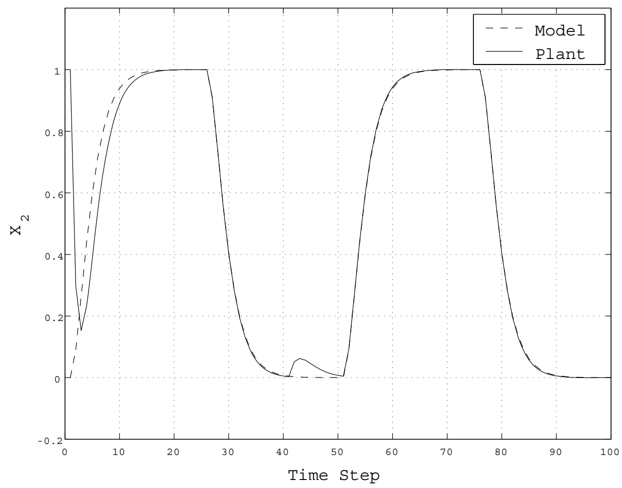

Fig. 6 Tracking Control of the Lorenz system

V. CONCLUSION

In this paper, a novel design method for the control of chaotic dynamical systems has been presented. It has been shown that the nonlinear part of the chaotic dynamical system can be estimated by the RBFNs. The simulation experiments have illustrates that the proposed method is effective for the model-following control of the chaotic systems.

ACKNOWLEDGMENT

The authors thank Dr. T. Murakami for many helpful comments.

REFERENCES

[1] S. Haykin, *Neural Networks – A Comprehensive Foundation*, Macmillan, New York, 1994.
[2] D. E. Rumelhart, G. E. Hinton and R. J. Williams, "Learning internal representations by error propagation," in Parallel Distributed Processing: Explorations in the Microstructure of Cognition, D. E. Rumelhart and J. L. McClelland, eds., vol. 1, chapter 8, Cambridge, MA: MIT Press, 1986.
[3] K. S. Narendra and K. Parthasarathy, "Identification and control of dynamical systems using neural networks," IEEE Trans. Neural Networks, vol. 1, no. 1, pp. 4-27, 1990.
[4] P. D. Wasserman, Advanced Method in Neural Networks, Van Nostrand Reinhold, New York, pp. 147-176, 1993.
[5] D. Sbarbaro, J. P. Segovia, S. Alcozer and J. Gonzales, "Applications of radial basis network technology to process control," IEEE Trans. Control Systems Technology, vol. 8, no. 1, pp. 14-22, 2000.
[6] K. B. Kim, J. B. Park, Y. H. Choi and G. Chen, "Control of chaotic dynamical systems using radial basis function approximators," Information Sciences, vol. 130, pp. 165-183, 2000.
[7] G. H. Golub and C. F. Van-Loan, Matrix Computation, 3rd Edition, The Johns Hopkins Univ. Press, Baltimore and London, 1996.
[8] G. F. Franklin, J. David Powell and Michael L. Workman, Digital Control of Dynamic Systems, Addison-Wesley, New York, 1990.

Yoichi Ishikawa was born in Kanagawa, Japan, on August 4, 1981. He received the B. E. degree in Electronics and Communications from Meiji University, Kawasaki, Japan, in 2005. He is currently working toward the M. E. degree at Graduate School of Electrical Engineering, Meiji University. His research interests include digital control and signal processing.

Yuichi Masukake was born in Chiba, Japan, on October 26, 1983. He is currently working toward the B. E. degree in Electronics and Communications Meiji University. His research interests include digital signal processing and its applications.

Yoshihisa Ishida was born in Tokyo, Japan, on February 24, 1947. He received the B. E., M. E., and Dr. Eng. Degrees in Electrical Engineering, Meiji University, Kawasaki, Japan, in 1970, 1972, and 1978., respectively. In Meiji University, as a Research Assistant and became a Lecturer and an Associate Professor in 1978 and 1981, respectively. He is currently a Professor at the Department of Electronics and Communications, Meiji University. His current research interests include signal processing, speech analysis and recognition, and digital control. He is a member of the IEEE, and the IEICE of Japan.